THE JOURNAL OF PHYSICAL CHEMISTRY C LETTERS

2009, *113,* 3382–3385
Published on Web 02/11/2009

Nature of Ti Interstitials in Reduced Bulk Anatase and Rutile TiO_2

Emanuele Finazzi, Cristiana Di Valentin,* and Gianfranco Pacchioni

Dipartimento di Scienza dei Materiali, Università di Milano-Bicocca, Via R. Cozzi, 53 20125, Milano, Italy

Received: December 18, 2008; Revised Manuscript Received: February 2, 2009

The preferred charge and spin state of an interstitial (Ti_{int}) atom in reduced bulk rutile or anatase $Ti_{1+x}O_2$ has been investigated with spin-polarized hybrid density functional theory (DFT) calculations. A neutral Ti_{int} placed in an interstitial cavity of titania spontaneously transforms into a Ti^{3+} ion with nearly one electron localized on the 3d shell; the remaining three electrons are donated to the lattice Ti ions. Spin polarization is essential to obtain a correct description of the electronic structure of the defect.

Titanium dioxide is a versatile material used in photocatalysis, self-cleaning coatings, solar cells, and so forth.[1] It is often in reduced form (i.e., the stoichiomety is such that Ti is in excess with respect to O[2,3]); this can result in samples with the chemical formula TiO_{2-x} (O vacancies, V_O) or $Ti_{1+x}O_2$ (Ti interstitials, Ti_{int}). The common feature is that in both cases reduction is accompanied by the appearance of Ti^{3+} species, which play an important role in the optical and chemical activities of the material. The fingerprint of the formation of Ti^{3+} ions is a gap state ~2 eV above the valence band (VB) maximum and ~1 eV below the conduction band (CB) minimum, as probed by photoelectron spectroscopy[4−6] and electron energy loss experiments.[7] Other spectroscopic features of reduced TiO_2 are (i) the sample's blue color (whose intensity is a measure of the level of reduction) assigned to d−d transitions,[8] (ii) the EPR-measured g tensor typical of a Ti $3d^1$ state,[9−11] and (iii) the shift in the core-level binding energies of the Ti atoms.[12] The nature of reduced titania (V_O or Ti_{int}) is still controversial. Different studies have shed light on the role of each of these point defects;[3,13] according to Henderson,[14] the major diffusing species in the bulk-assisted reoxidation of ion-sputtered TiO_2 surfaces are Ti_{int} rather than V_O centers. More recently, by combining STM and photoelectron spectroscopy measurements, it has been proposed that Ti_{int} in the near-surface region is largely responsible for the defect state in the band gap.[15] The two defects probably coexist but in different concentrations, depending on the history of the sample, chemical synthesis, thermal treatment, and so forth.

It is thus important to provide a detailed description of the electronic structure of both defects, V_O and Ti_{int}. Unfortunately, this represents a challenge for theory[3] and, in particular, for DFT-based approaches.[16,17] Because of the insufficient cancelation of the self-interaction energy in pure DFT functionals, V_O centers in TiO_2 are described as fully delocalized, and the corresponding one-electron energy state is at the bottom of the CB, not in the gap at variance with the experiment.[6,15,16] The introduction of a Hubbard term (GGA+U) or of an admixture of Hartree−Fock (HF) exchange in DFT significantly improves the description of the Ti $3d^1$ defect states and allows us to induce the polaronic distortion around the defect, which is the origin of localization.[15,16,18,19] It must be stressed that the electronic structure in DFT is computed at 0 K and that partial or full delocalization can occur at finite temperatures, an aspect that must be taken into account when comparing theoretical with experimental findings.[20] In fact, because of the small energy barrier for electron hopping, at RT the mobility of the polaron associated with the Ti^{3+} species is non-negligible.[21]

We present a detailed analysis of the nature of a Ti_{int} impurity in bulk anatase and rutile TiO_2 on the basis of pure and hybrid DFT calculations. Most of the work performed on Ti interstitials on the rutile (110) surface[22] or in bulk rutile[14,23−25] or anatase[26,27] used LDA[25,23,21] or GGA[14,22,24,26] non -spin-polarized approaches. Only recently was the study on Ti atoms adsorbed on the rutile (110) surface done using a spin-polarized and DFT+U approach.[6] Of course, spin-polarization is indispensable when discussing the spin state of the bulk Ti_{int} species. In fact, we will show that a neutral Ti atom inserted into an interstitial cavity in bulk anatase or rutile spontaneously forms a Ti^{3+} ($3d^1$) interstitial and donates the remaining three valence electrons to neighboring lattice Ti ions ($Ti_{lattice}$), giving rise to specific magnetic states in the band gap of the material. We will also show that self-interaction corrected functionals are needed to describe properly the localized nature and the polaronic distortion of the defect states resulting from Ti addition.

Spin-polarization calculations have been performed within the generalized gradient approximation (GGA) using the PBE[28] functional or the B3LYP hybrid functional,[29,30] where 20% of the exact HF exchange is mixed in with the DFT exchange. We checked the effect of varying the amount of HF exchange on the results by also using 10% (HF10) or 30% (HF30) HF exchange (Supporting Information). The Kohn−Sham orbitals are expanded in Gaussian-type orbitals (GTO), as implemented in the CRYSTAL06 code[31] (the all-electron basis-sets are Ti 86411(d41)[32] and O 8411(d1)[33]). For an improved description of Ti^{3+}, we added a diffuse d function ($\alpha = 0.13$). To model a Ti_{int} species, we included a neutral Ti atom in an interstitial site of the nearly cubic $2\sqrt{2} \times 2\sqrt{2} \times 1$ anatase (96 + 1 atoms) and $2 \times 2 \times 3$ rutile (72 + 1 atoms) supercells. The optimized bulk lattice parameters were taken from previous PBE (anatase: $a = 3.786$ Å, $c = 9.737$ Å; rutile: $a = 4.634$ Å, $c = 2.963$ Å)[34] and B3LYP (anatase: $a = 3.776$ Å, $c = 9.866$ Å; rutile: $a = 4.5477$ Å, $c = 2.9407$ Å)[35] calculations. Full geometry

* Corresponding author. E-mail: cristiana.divalentin@mater.unimib.it.

10.1021/jp8111793 CCC: $40.75

optimization was performed until the largest component of the ionic forces was less than 5×10^{-4} au. The k-space sampling was restricted to the Γ point. The total and projected densities of states (DOS and PDOS) have been obtained with a 36 k-points mesh.

We start with a discussion of bulk anatase. Here, a Ti_{int} atom (valence configuration $3d^24s^2$) was placed in the center of a pseudo-octahedral position (Figure 1), and the structure was fully optimized. Because a neutral Ti is potentially a 1-, 2-, 3-, or 4-electron donor, the final spin multiplicity and oxidation state after structural relaxation are not a priori defined. Three spin-state configurations have been considered (i.e., singlet closed shell ($S = 0$), triplet (two unpaired electrons, $S = 1$), and quintet (four unpaired electrons, $S = 2$).

For all of the spin configurations and functionals, we found that the top apical oxygen atom of the pseudo-octahedral site (Figure 1 and Table S1) moves toward the Ti_{int} atom, resulting in a rather short $Ti_{int}-O$ bond (1.939 Å for B3LYP and $S = 2$). On the contrary, the distance of Ti_{int} from the opposite O in the bottom axial position is considerably increased (3.460 Å for B3LYP and $S = 2$). The final coordination of the Ti_{int} species is thus quasi-pyramidal. For comparison, the B3LYP $Ti_{lattice}-O$ distances for stoichiometric bulk anatase are 1.940 Å ($Ti-O_{eq}$) and 2.020 Å ($Ti-O_{ax}$).

Without spin polarization ($S = 0$) all electrons are forced to pair up. The hybrid functionals show the formation of a doubly occupied defect state, which is well separated from the bottom of the CB (Figure 1) with nearly one electron localized on the 3d levels of Ti_{int} and the second electron shared by two next-neighbor $Ti_{lattice}$ ions. The two electrons are singlet coupled. A second electronic state appears at the bottom of the CB and is delocalized on a number of $Ti_{lattice}$ ions, which are only partially reduced. Forcing the spins to be paired, however, results in a configuration that is 0.78 eV higher than the open-shell triplet ($S = 1$, B3LYP). Here, one of the two unpaired electrons is almost entirely localized on Ti_{int}, and the second one is localized on a close $Ti_{lattice}$ ion (Ti_b, Figure 1). The remaining two extra electrons are coupled in a state that is delocalized on various $Ti_{lattice}$ atoms. Therefore, as soon as the constraint on the spin is released, the Ti_{int} species spontaneously donates three electrons to the surroundings, forming a Ti^{3+} ($3d^1$) ion. Increasing the amount of HF exchange in the exchange-correlation functional has the effect of increasing the level of localization on the Ti lattice ions (and vice versa), but the general picture does not change. The positions of the Ti_{int} and $Ti_{lattice}$ 3d states are about 2.75 eV above the VB and 0.70 eV below the CB (the gap in B3LYP is partially overestimated, being 3.9 eV; see Figure 1; this means that the position of the levels in the DOS plots has to be scaled by ~20% in order to be compared with experimental measurements).

For the highest spin multiplicity ($S = 2$), we also considered the standard PBE functional to determine if the HF exchange is essential to achieve localization on Ti_{int}, as shown for the oxygen vacancy in rutile TiO_2.[15] Both methods, PBE and B3LYP, show the formation of a Ti_{int} ion in the +3 oxidation state with one electron in the 3d shell. (The spin populations are $0.61e^-$ in PBE and $0.86e^-$ in B3LYP.) The result is interesting because it demonstrates that the Ti_{int} species occupies a low-symmetry environment that stabilizes the localized state (small polaron) independently of the functional used, a result that provides strong support to this conclusion. The remaining three excess electrons derived from Ti_{int} are delocalized on several $Ti_{lattice}$ atoms, in particular, those closer to Ti_{int} (Ti_a, Ti_b, and Ti_c; Tables 1 and S2). We call this solution B3LYP-A. Also,

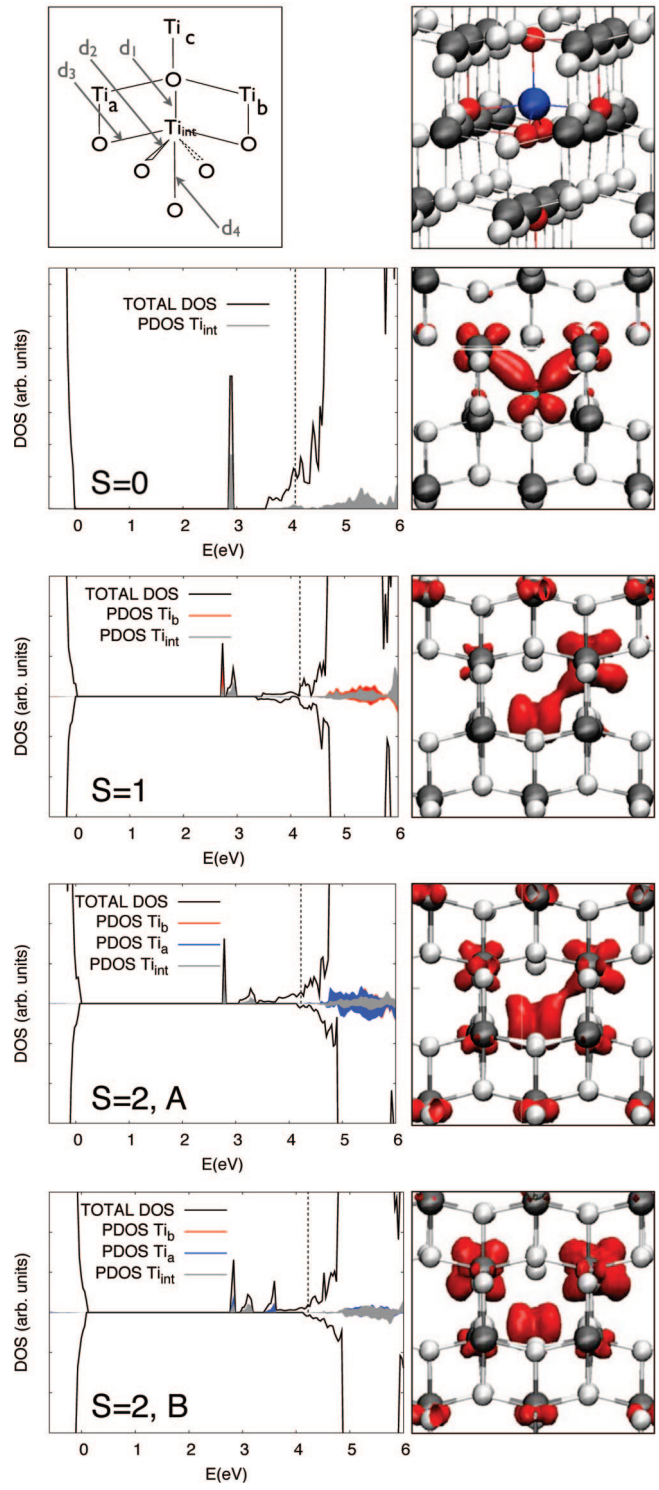

Figure 1. Anatase bulk. (Top) Schematic (left) and ball-and-stick (right) representations of the Ti_{int} (blue) pseudo-octahedrally coordinated to six O atoms (red). White spheres are the remaining O atoms, and dark-gray spheres are $Ti_{lattice}$ ions. (Left) B3LYP total and projected (on Ti_{int}, $Ti_{lattice(a)}$, and $Ti_{lattice(b)}$) DOS of the $S = 0$, 1, 2 spin configurations. The dotted line represents the Fermi energy. (Right) Corresponding electron ($S = 0$) and spin ($S = 1$, 2) density plots.

in this case the extent of localization on the $Ti_{lattice}$ ions increases by increasing the amount of HF exchange. The occupied defect states lie approximately 2.8 eV above the top of the VB (B3LYP). There is also another nearly degenerate solution, B3LYP-B, that is only 0.04 eV higher in energy than the B3LYP-A solution, where two out of the three electrons

TABLE 1: Atomic Spin Population ($S = 2$) on Ti_{int} and Next-Neighbor $Ti_{lattice}$ Ions for Bulk Anatase and Rutile as Defined in Figures 1 and 2

anatase	Ti_{int}	$Ti_{lattice}(a)$	$Ti_{lattice}(b)$	$Ti_{lattice}(c)$
PBE	0.61	0.35	0.35	0.12
B3LYP-A	0.86	0.27	0.36	0.13
B3LYP-B	0.76	0.73	0.73	0.06
rutile	Ti_{int}	$Ti_{lattice(eq)}$	$Ti_{lattice(eq)}$	$Ti_{lattice(eq)}$
PBE	0.31	0.19	0.20	0.20
B3LYP	0.71	0.80	0.67	0.72

transferred to $Ti_{lattice}$ ions are fully localized (on Ti_a and Ti_b). In the DOS of Figure 1, this translates into three localized states in the band gap separated by about 0.8 eV. This is an important observation. It shows that, although some mixing is present and Ti_{int} species introduce new gap states well below the CB, localization on $Ti_{lattice}$ ions results in more shallow states that are closer to the bottom of the CB. The electron localization on $Ti_{lattice}$ ions of anatase is a delicate issue that depends on the possibility of inducing a local lattice distortion and trapping the electron in a single 3d orbital. It costs almost no energy to detrap this electron and transfer it to a more delocalized state.

Of the electronic configurations considered, the singlet ($S = 0$) is definitely the least stable, but the triplet ($S = 1$) and quintet ($S = 2$) configurations are within 0.1 eV (the triplet is slightly more stable). This confirms the tendency of the Ti_{int} ion to assume the +3 ($3d^1$) oxidation state whereas the spin coupling of the other electrons transferred to the $Ti_{lattice}$ ions is much less important for the total stability because their exchange interaction is small.

On the basis of this conclusion, for bulk rutile we considered only the highest spin state ($S = 2$) using both hybrid and PBE functionals. Unlike anatase, in rutile the Ti_{int} atom is located in a pseudo-octahedral site (Figure 2) that is only slightly distorted after geometry optimization. As for anatase, the Ti_{int} neutral atom donates three electrons to the host crystal and transforms

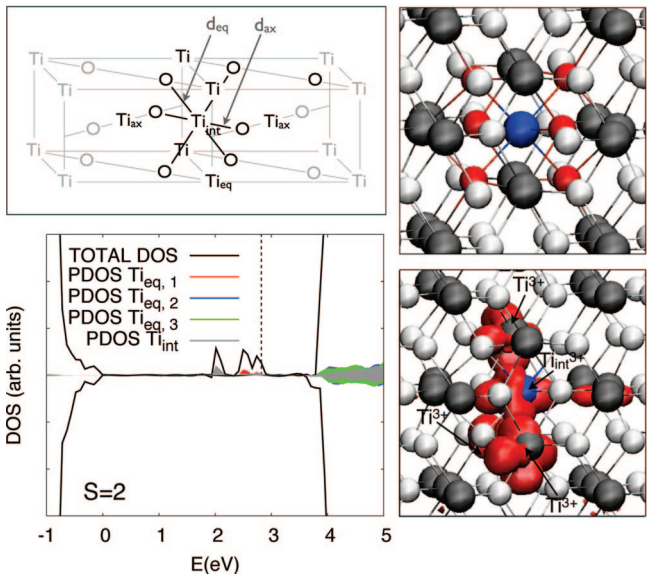

Figure 2. Rutile bulk. (Top) Schematic (left) and ball-and-stick (right) representations of the Ti_{int} (blue) pseudo-octahedrally coordinated to six O atoms (red). White spheres are the remaining O atoms and dark gray spheres are $Ti_{lattice}$ ions. (Left) B3LYP total and projected (on Ti_{int} and three $Ti_{lattice(eq)}$) DOS of the $S = 2$ spin configuration. The dotted line represents the Fermi energy. (Right) Corresponding spin density plots.

to a Ti^{3+} $3d^1$ ion. The remaining electrons are distributed on $Ti_{lattice}$ ions with a level of localization that partially depends on the functional used. At the HF30 level, all four unpaired electrons are almost entirely localized (Table S5 and Figure S4). In B3LYP, the degree of localization is less pronounced (Table 1), and the spin is partially delocalized on a larger number of Ti ions beyond the nearest neighbors of Ti_{int}. The defect states are in the band gap 1.1−1.8 eV from the bottom of the CB (Figure 2); as in anatase and in rutile Ti_{int}, the localized states in the band gap are within a window of 0.8 eV. With the PBE functional, there is only a small localization on Ti_{int} ($0.31e^-$, Table 1), resulting in a tiny feature just below the bottom of the CB (Figure S4); the remaining electrons are delocalized over several $Ti_{lattice}$ ions (Table S5).

To summarize, we have introduced a neutral Ti atom into the interstitial cavities of stoichiometric anatase and rutile TiO_2 crystals, and we have considered the resulting electronic structure. The Ti_{int} atom spontaneously donates three electrons to the surrounding lattice Ti ions and forms a Ti^{3+} ion with a single electron localized on a 3d shell. This result is obtained in both anatase and rutile and with pure and hybrid functionals, although the extent of localization is different in the two approaches. The reason is that the interstitial cavity provides a kind of natural polaronic distortion that favors localization on Ti_{int}. It is interesting that on the (110) rutile surface the addition of a neutral Ti atom results in the formation of a Ti^{2+} ($3d^2$) adsorbed species, not Ti^{3+}.[6] As a consequence of the electron transfer, other lattice Ti ions are chemically reduced. However, in this case the level of localization depends on the possibility of inducing a polaronic distortion of the pseudo-octahedral environment, as discussed in the literature.[15] This distortion is more easily obtained with hybrid methods and, in particular, for higher portions of HF exchange. The formation of interstitial Ti^{3+} ($3d^1$) ions is found only when a spin-polarized calculation is performed; the use of a non-spin-polarized approach in fact results in a doubly occupied state that does not account for the observation of the EPR signal[9−11] and leads to a higher total energy. The presence of both lattice and interstitial Ti^{3+} ions results in new states in the band gap, about 1−1.5 eV below the CB. Because these states are associated with different local environments, the corresponding energy levels are not at the same position but are distributed in an interval of 0.7−0.8 eV, with Ti_{int} ions largely responsible for the deepest states. This is not in contradiction with the experimental observation of a single peak in UPS or EELS experiments: the observed peaks are in fact rather broad (typical fwhm of 0.5 eV) and may well be due to the convolution of more than a single peak. It is also possible, however, that the observation of the more shallow states mostly associated with $Ti_{lattice}$ species can be observed only at rather low temperatures.

Acknowledgment. This work has been supported by the Italian MIUR through a PRIN 2005 project and the COST Action D41 "Inorganic oxide surfaces and interfaces". We are grateful to Professor A. Selloni for helpful discussions.

Supporting Information Available: Structural data, spin population, and relative stability of the solutions obtained with PBE and hybrid (B3LYP, H10, and H30) functionals. DOS and PDOS for all spin states and functionals considered. This material is available free of charge via the Internet at http://pubs.acs.org.

References and Notes

(1) Chen, X.; Mao, S. S. *Chem. Rev.* **2007**, *107*, 2891.
(2) Thompson, T. L.; Yates, J. T., Jr. *Chem. Rev.* **2006**, *106*, 4428.
(3) Ganduglia-Pirovano, M. V.; Hofman, A.; Sauer, J. *Surf. Sci. Rep.* **2007**, *62*, 219.
(4) Henrich, V. E.; Dresselhaus, G.; Zeiger, H. J. *Phys. Rev. Lett.* **1976**, *36*, 1335.
(5) Kurtz, R. L.; Stock-Bauer, R.; Madey, T. E. *Surf. Sci.* **1989**, *218*, 178.
(6) Nolan, M.; Elliot, S. D.; Mulley, J. S.; Bennet, R. A.; Basham, M.; Mulheran, P. *Phys. Rev. B* **2008**, *77*, 235424.
(7) Henderson, M. A.; Epling, W. S.; Peden, C. H. F.; Perkins, C. L. *J. Phys. Chem. B* **2003**, *107*, 534.
(8) Khomenko, V. M.; Langer, K.; Rager, H.; Fett, A. *Phys. Chem. Mineral* **1998**, *25*, 338.
(9) Serwicka, E.; Schierkamp, M. W.; Schindler, R. N. *Z. Naturforsch.* **1981**, *36a*, 226.
(10) Chester, P. F. *J. Appl. Phys.* **1961**, *32*, 2233.
(11) Sekiya, T.; Yagisawa, T.; Kamiya, N.; Mulmi, D. D.; Kurita, S.; Murakami, Y.; Kodaira, T. *J. Phys. Soc. Jpn.* **2004**, *73*, 703.
(12) Nerlov, J.; Christensen, S. V.; Wichel, S.; Pedersen, E. H.; Møller, P. J. *Surf. Sci.* **1997**, *371*, 321.
(13) Diebold, U. *Surf. Sci. Rep.* **2003**, *48*, 53.
(14) Henderson, M. A. *Surf. Sci.* **1999**, *419*, 174.
(15) Wendt, S.; Sprunger, P. T.; Lira, E.; Madsen, G. K. H. M.; Li, Z.; Hansen, J.; Matthiensen, J.; Blekinge-Rasmussen, A.; Lægsgaard, E.; Hammer, B.; Besenbacher, F. *Science* **2008**, *320*, 1755.
(16) Di Valentin, C.; Pacchioni, G.; Selloni, A. *Phys. Rev. Lett.* **2006**, *97*, 166803.
(17) Finazzi, E.; Di Valentin, C.; Pacchioni, G.; Selloni, A. *J. Chem. Phys.* **2008**, *129*, 154113.
(18) Calzado, C. J.; Hernández, N. C.; Sanz, J. F. *Phys. Rev. B* **2008**, *77*, 045118.
(19) Morgan, B. J.; Watson, G. W. *Surf. Sci.* **2007**, *601*, 5034.
(20) Krüger, P.; Bourgeois, S.; Domenichini, B.; Magnan, H.; Chandesris, D.; Le Fevre, P.; Flank, A. M.; Jupille, J.; Floreano, L.; Cossaro, A.; Verdini, A.; Morgante, A. *Phys. Rev. Lett.* **2008**, *100*, 055501.
(21) Deskins, N. A.; Dupuis, M. *Phys. Rev. B* **2007**, *75*, 195212.
(22) Park, K. T.; Pan, M.; Meunier, V.; Plummer, E. W. *Phys. Rev. B* **2007**, *75*, 245415.
(23) He, J.; Sinnott, S. B. *J. Am. Ceram. Soc.* **2005**, *88*, 737.
(24) Cho, E. J.; Han, S.; Ahn, H.-S.; Lee, K.-R.; Kim, S. K.; Hwang, C. S. *Phys. Rev. B* **2006**, *73*, 193202.
(25) Iddir, H.; Ogut, S.; Zapol, P.; Browning, N. D. *Phys. Rev. B* **2007**, *75*, 073203.
(26) Na-Phattalung, S.; Smith, M. F.; Kim, K.; Du, M.-H.; Wei, S.-H.; Zhang, S. B.; Limpijumnong, S. *Phys. Rev. B* **2006**, *73*, 125205.
(27) Zuo, X.; Yoon, S.-D.; Yang, A.; Vittoria, C.; Harris, V. G. *J. Appl. Phys.* **2008**, *103*, 07B911.
(28) Perdew, J. P.; Burke, K.; Ernzerhof, M. *Phys. Rev. Lett.* **1996**, *77*, 3865.
(29) Becke, A. D. *J. Chem. Phys.* **1993**, *98*, 5648.
(30) Lee, C.; Yang, W.; Parr, R. G. *Phys. Rev. B* **1998**, *37*, 785.
(31) Saunders, V. R.; Dovesi, R.; Roetti, C.; Orlando, R.; Zicovich-Wilson, C. M.; Harrison, N. M.; Doll, K.; Civalleri, B.; Bush, I. J.; D'Arco, Ph.; Llunell, M. *CRYSTAL03 User's Manual*; University of Torino: Torino, Italy, 2003.
(32) Zicovich-Wilson, C. M.; Dovesi, R. *J. Phys. Chem. B* **1998**, *102*, 1411.
(33) Muscat, E. J. Ph.D. Thesis, University of Manchester, 1998, with an additional d function (exponent 0.6).
(34) Lazzeri, M.; Vittadini, A.; Selloni, A. *Phys. Rev. B* **2001**, *63*, 155409.
(35) Zhang, Y.; Lin, W.; Li, Y.; Ding, K. N.; Li, J. Q. *J. Phys. Chem. B* **2005**, *109*, 19270.

JP8111793